Advances in Environmental Technology 11(2) 2025, 193-206.

Iranian Reasearch Organization for Science and Technology (IROST)

Advances in Environmental Technology

Journal home page: https://aet.irost.ir

Thermal activation and loading of Clay/TiO_2/CTAB composite: physicochemical characterization and adsorption-photodegradation of methyl orange

Nohong Nohong[a], Juneti Tandi Limbong Baratau[a], Dwiprayogo Wibowo[b], Faizal Mustapa[c], Ahmad Zulfan[d], Maulidiyah Maulidiyah[a], Muhammad Nurdin*[a]

[a]*Department of Chemistry, Universitas Halu Oleo, Kendari, Indonesia.*

[b]*Department of Environmental Engineering, Universitas Muhammadiyah Kendari, Kendari, Indonesia.*

[c]*Marine Science, Institut Teknologi & Bisnis Muhammadiyah Kolaka, Kolaka, Indonesia.*

[d]*Nickel Research Institute, Universitas Muhammadiyah Kendari, Kendari, Indonesia.*

ARTICLE INFO

Document Type:
Case Study

Article history:
Received 14 July 2024
Received in revised form
30 January 2025
Accepted 01 February 2025

Keywords:
Clay
TiO_2
CTAB
Photodegradation
Adsorption

ABSTRACT

The discharge of textile effluents induces organic pollutants that necessitate attention to ensure environmental sustainability. This study presents eco-synthesis and an enhanced adsorption-photocatalyst over a Clay/TiO_2/CTAB composite for photodegradation of an organic dye pollutant (Methyl Orange; MO). Natural clay used in this work was purified via hydrothermal treatment to produce activated clay. Subsequently, TiO_2 was intercalated with CTAB surfactant and combined with clay to obtain the Clay/TiO_2/CTAB composite. The material was synthesized via a dispersion and centrifugation process. The presence of TiO_2 pillared Clay/CTAB showed important photocatalytic properties and high-adsorption performance for the degradation of the MO compound. The Clay/TiO_2/CTAB was found to be the most effective adsorption-photocatalyst when compared using homogeneous material. The natural clay was characterized by X-ray fluorescence (XRF), while Clay/TiO_2/CTAB was identified using X-ray diffraction (XRD), Fourier transform infrared spectroscopy (FTIR), and scanning electron microscope (SEM). The successful formation of the Clay/TiO_2/CTAB was indicated by FTIR analysis under the wavenumber shown in the fingerprint region predicting the presence of Al-OH and O-Ti-O elements (450-1000 cm-1), while CTAB was generalized to form amide bonds (1360 cm-1). Confirmation of the XRF data shows Clay contains high SiO_2 and Al_2O_3 with good crystallinity, as well as Clay/TiO_2 and Clay/TiO_2/CTAB, showing crystallinity patterns of quartz, kaolinite, anatase, rutile, and montmorillonite. The micrographs of the synthesized materials show rough surfaces and non-uniform surfaces with different TiO_2 grains widely dispersed on the surface. The adsorption-photocatalyst performance of

*Corresponding author Tel.:
E-mail: muhammad.nurdin@uho.ac.id
DOI: 10.22104/AET.2025.6993.1920

the Clay/TiO_2/CTAB composite was evaluated in three parameters, namely pH optimization, contact time, and degradation ability, showing excellent degradation performance at a pH 5 with 60 minutes contact time with a degradation efficiency of 89.90%. Clay/TiO_2/CTAB material influenced the adsorption ability and changed the acidity of the waste to make the treated wastewater environmentally safe.

1. Introduction

In recent years, river water quality in most parts of Indonesia has significantly deteriorated, particularly after passing through residential, industrial, and agricultural areas [1-3]. In developing countries, including Indonesia, domestic sewage constitutes the largest source of pollution, accounting for approximately 75% of source water contamination [4]. Industrial wastewater also presents a significant environmental challenge [5, 6]. Improper treatment and management of liquid waste can severely impact the environment, especially water resources. Water pollution caused by toxic compounds, such as heavy metal ions and dyes, is detrimental to the ecology and poses a significant threat to human health and the environment [7, 8]. The textile industry is a major global polluter, second only to the petroleum industry [9, 10]. Numerous studies have reported that hazardous chemical compounds from textile industry processing have polluted several rivers in Indonesia, including the Cikijing [11, 12], Cipeusing [13], Brantas, and Bengawan Solo [14]. Despite the domestic textile industry recording an export growth of US$12.4 billion, a 6% increase from the previous year's US$11.8 billion, it continues to have a significant impact on environmental pollution [15]. The main factors contributing to environmental damage from the textile industry are dye compounds, as they contain a wide range of hazardous chemicals in both low and high concentrations [16, 17]. Some of these dyes are toxic and exhibit carcinogenic and mutagenic effects on both aquatic life and humans [18, 19]. Textile dyes are typically derived from azo compounds and their derivatives, which include benzene groups that are notoriously difficult to degrade [20, 21]. The prolonged presence of azo compounds in the environment can lead to diseases due to their toxic and mutagenic properties [22].

One commonly used azo dye in the textile industry is methyl orange (MO), which is extensively employed as a dyeing agent and as an indicator in acid-base titrations [23]. MO textile dyes are categorized as non-biodegradable pollutants [24]. Waste dyes from various industries are notably stable and resistant to biodegradation due to their complex aromatic molecular structures [8].

Several technologies have been applied to treat dye effluents, including chlorination, adsorption, biodegradation, and ozonation [25, 26]. While these methods can be effective, they often incur significant operational costs and may result in new environmental issues, such as the formation of secondary pollutants. Among the various developed processes, photodegradation emerges as a promising alternative due to its simplicity, efficiency, and widespread availability [27, 28]. Conventional TiO_2 photocatalysts have been extensively researched for their excellent photoactivity, stability, and non-toxicity [29, 30]. However, due to the 3.2 eV band gap of TiO_2, these photocatalysts are only active under UV light irradiation, which constitutes a mere 4% of total sunlight, thus severely limiting their practical applications [31]. Consequently, research has increasingly focused on the development of highly efficient visible light-based photocatalysts.

Research on TiO_2-pillared clay presents promising prospects due to the extensive use of TiO_2 as a catalyst. Ulhaq et al. [32] reported a 93% removal of hydrocarbon pollutants from petroleum refinery wastewater through simultaneous photocatalytic oxidation and adsorption using TiO_2/CTAB-Bt under UV light. Similarly, Yuan et al. [33] demonstrated that Clay/TiO_2/CTAB based on TiCl4 and applied with diethanolamine (DEA) as a dispersant exhibited a 10% higher photocatalytic efficiency compared to TiO_2-P25. In their study, the use of TiO_2-P25 as a pillaring agent increased the basal spacing of the clays, with the metal oxide

distributed on the pillared clay layer, thereby increasing the acidity of the clays.

Further research employing surfactants such as cetyl-trimethyl ammonium bromide (CTAB) aims to enhance the intercalation of TiO_2 metal oxide, resulting in pillared clays with larger basal spacing and more uniform pore distribution [34, 35]. This improved intercalation not only has the potential to increase the efficiency of capturing and degrading contaminants from industrial waste but also paves the way for new applications in more sustainable and effective waste treatment [33]. Surfactants like CTAB facilitate increased spacing between clay layers, which enhances the uptake and degradation of contaminants. With increased basal spacing and more uniform pore distribution, these pillared clays can function more effectively as media for photocatalysis, offering a more environmentally friendly solution to water pollution problems [36, 37].

The synergistic effects of Clay/TiO_2/CTAB present a promising and cost-effective approach to addressing wastewater treatment in an efficient and environmentally friendly manner. The integration of TiO_2 with carrier materials enhances the effectiveness of photodegradation, providing a more sustainable and efficient method to mitigate water pollution [38]. The CTAB surfactant increases the spacing between clay layers, facilitating more efficient uptake and degradation of contaminants [39]. With increased basal spacing and more uniform pore distribution, these pillared clays serve as highly effective media for photocatalysis, offering an environmentally friendly solution to water pollution issues.

Interdisciplinary studies are crucial for overcoming challenges in wastewater treatment and ensuring the application of these technologies in sustainable water resource management. This research focuses on the synthesis and application of TiO_2-pillared clays, particularly using surfactants to enhance photocatalytic performance, demonstrating significant potential in addressing environmental pollution. By continuing to innovate in sewage treatment technologies, it is possible to develop wastewater treatment systems that are not only effective but also sustainable, thereby reducing the negative impact of industrial activities on the environment and supporting the preservation of water resources for future generations.

2. Experimental Methods

2.1. Clay Preparation and Activation

The clay, sourced from the North Konawe Regency in Southeast Sulawesi, Indonesia, was purified by removing coarse particles through multiple washings with distilled water. After cleaning, the clay was air-dried in direct sunlight for five days and subsequently oven-dried to eliminate any remaining moisture. The dried clay was finely ground to a particle size of 180 mesh using an agate mortar. Following this preparation, the fine clay underwent physical (thermal) activation. Specifically, 200 grams of fine clay was calcined at 600°C for four hours to reduce the moisture content, which involves the removal of hydroxyl groups from the clay structure. In addition, this treatment increased the surface area of the activated clay to evaluate its potential to improve the mechanical properties of the composite.

2.2. Synthesis of Clay/TiO_2/CTAB

This study utilized TiO_2 Degussa-P25 for a synergistic combination with CTAB and activated clay. Initially, TiO_2/CTAB was prepared by dissolving 0.5 grams of TiO_2-P25 in 2.0 mL of ethanol (P.A.). The CTAB solution variations were prepared at concentrations of 1.0 mM, 2.0 mM, and 3.0 mM. Each mixture was stirred using a magnetic stirrer for two hours at a stirring speed of 100 rpm at 80°C to obtain the TiO_2/CTAB material. For the synthesis of the Clay/TiO_2/CTAB material, 1.0 g of activated clay was dispersed into 100 mL of distilled water and stirred using a magnetic stirrer for five hours. Subsequently, 0.5 g of the TiO_2/CTAB pillar agent was slowly added to the suspended solution and stirred for 24 hours. The resulting suspension was separated using a centrifuge and washed with distilled water. The suspended solids in the form of Clay/TiO_2/CTAB were dried in an oven for two hours at 105°C. Finally, the Clay/TiO_2/CTAB was finely crushed and sieved using a 100-mesh sieve, making it ready for testing with the MO test compound.

2.3. Material Characterizations

Several instruments were used for material characterization to confirm the successful

synthesis of the Clay/TiO_2/CTAB composite, including XRF (Bruker-S2 Puma), FTIR (Shimadzu-IR Prestige 21), XRD (PANalytical X'Pert-PRO), and SEM (FEI-Inspect-S50). XRF was employed to identify chemical elements in the clays before and after activation. FTIR was used to identify functional groups after the material synthesis process by comparing the absorption at the wave number formed between Clay, TiO_2/CTAB, and Clay/TiO_2/CTAB. XRD was used to evaluate the crystallinity and phase composition of the materials, while SEM provided detailed information on the morphology, porosity, and particle size distribution in the Clay/TiO_2/CTAB composite.

2.4. Removal of MO Dye Compound

The removal of the MO dye compound using Clay/TiO_2/CTAB was conducted with various testing parameters, including optimization of pH, contact time, and the effect of concentration on the MO compound. For pH optimization, 10 mL of the MO compound solution with pH variations of 1.0, 3.0, 5.0, 7.0, 9.0, and 11.0 was added to a 100 mL beaker. The pH was adjusted using 0.1 M NaOH or HCl and monitored with a pH meter. Clay/TiO_2/CTAB material was added to each beaker and stirred for 60 minutes. The solution and material were separated by decantation and analyzed using a UV-Vis spectrophotometer. The optimum pH was determined by comparing the amount of MO to the ability to reduce the concentration of the MO compound. Contact time optimization involved varying the contact time to 30, 60, 90, 120, 150, and 180 minutes using 100 mL of 25 $mg.L^{-1}$ MO solution with 0.5 g of Clay/TiO_2/CTAB material. The ability to reduce MO concentration was recorded, and the degradation efficiency was identified. The effect of concentration on the MO compound was tested using concentrations of 5.0 $mg.L^{-1}$, 10.0 $mg.L^{-1}$, 15.0 $mg.L^{-1}$, 20.0 $mg.L^{-1}$, and 25.0 $mg.L^{-1}$, mixed with 0.5 g of Clay/TiO_2/CTAB material at the optimum contact time and pH. Each mixture was stirred using a magnetic stirrer under visible illumination and separated by decantation. The resulting filtrate was analyzed using a UV-Vis spectrophotometer.

3. Results and discussion

3.1. Clay Composition

The chemical composition of the clay was initially analyzed to determine the presence of minerals and to track any changes in mineral abundance due to temperature variations during the physical activation process. The data presented in Table 1 reveals that silica (SiO_2) and alumina (Al_2O_3) were present in substantial quantities, while other minerals were found in smaller amounts [40]. The behaviour of clays under thermal activation can be explained through thermal decomposition and phase transitions. High temperatures cause the decomposition of organic matter and bioinorganic compounds, leading to the release of gases such as CO_2 and H_2O. This process, known as dihydroxylation, results in weight reduction and resistance to decomposition, making them prominent in thermally activated clay. The enhanced binding capacity of oxygen atoms with rising temperature can be attributed to the increased reactivity of these minerals in their activated state. The observed changes in mineral abundance, as identified by XRF with increasing temperature, are linked to the loss-on-ignition (LoI) process. LoI explains how certain minerals enhance their ability to bind oxygen atoms (O_2) as the temperature increases. Additionally, some bioinorganic compounds in clays decompose at high temperatures, maintaining the stability and purity of minerals in their oxide forms [41]. Activated clays, with their large surface area and reactivity, effectively bind pollutants and facilitate various chemical reactions. This stability makes the material suitable for modifications with other compounds for environmental applications.

3.2. Material Characterizations

The synthesized material was characterized using FTIR, XRD, and SEM to confirm the successful incorporation of clay, TiO_2, and CTAB.

Table 1. Mineral identification in clay with thermal variations.

Elements / Oxides	Abundance (%)				
	Inactivated clay	500°C	550°C	600°C	650°C
SiO_2	63.12	66.61	67.03	66.68	67.23
TiO_2	0.63	0.64	0.64	0.64	0.63
Al_2O_3	17.56	19.99	19.86	19.09	20.45
CaO	0.26	0.28	0.30	0.28	0.28
K_2O	1.35	1.43	1.42	1.38	1.44
Cr_2O_3	0.12	0.11	0.11	0.12	0.11
MnO	0.04	0.04	0.04	0.04	0.04
Zn	<0.01	<0.01	<0.01	<0.01	<0.01
Ni	0.01	0.01	0.01	<0.01	0.01
Fe	5.50	4.84	4.90	4.94	4.89
Co	0.02	0.02	0.01	0.01	0.01
Na_2O	0.02	0.02	0.02	0.02	0.02
P_2O_5	0.01	0.01	0.01	0.01	0.01

FTIR analysis was used to identify the primary functional groups in Clay/TiO_2 and Clay/TiO_2/CTAB by comparing their specific absorption peaks. The samples primarily consist of oxide minerals, as evidenced by dominant absorption within the fingerprint region of 450-1000 cm^{-1} (Figure 1). Notable absorption peaks include 517, 694, 1041, 1469, 1619, 1890, 2374, 2931, 3432, and 3620 cm^{-1}. The sharp absorption at 517 cm^{-1} was associated with Ti-O bond vibrations within the TiO_2 lattice, confirming TiO_2 incorporation into the clay structure [42]. Key absorption bands at 3620, 3432, 1041, 1619-1890, and 2374 cm^{-1} corresponded to O-H stretching, Si-OH stretching, Si-O-Si stretching vibrations, Al-OH from bentonite clay and phosphate groups, indicating the presence of hydroxyl and silicate groups typical in clay minerals [32].

Additionally, the absorption at 2931 cm^{-1} suggested the presence of organic CH3 and CH2 groups, like from residual organic matter or surface modifications. A unique absorption at 1469 cm^{-1} differentiates Clay/TiO_2 from Clay/TiO_2/CTAB, revealing asymmetric bending vibrations of C-H in methyl and methylene groups or N-H bonded to ammonium groups, confirming the successful integration of cetyltrimethylammonium cations.

XRD patterns of Clay/TiO_2 and Clay/TiO_2/CTAB (Figure 2) show predominant peaks at 2θ values of 20.93, 26.66, and 50.19, confirming the presence of smectite mineral. Peaks at 2θ values of 25.23 (101), 37.71 (112), and 48.18 (200) correspond to the anatase phase of TiO_2. Isomorphic substitution in the clay structure, in which Al^{3+} replaces Si in the tetrahedral layer and Mg^{2+} substitutes in the octahedral layer, results in a net negative charge compensated by the adsorption of cations. This phenomenon supports cation exchange processes within the bentonite structure [32].

The hydrophilic nature of bentonite clay limits its adsorption of non-polar organic molecules. However, incorporating organic cations such as surfactants into the interlayers facilitates replacing inorganic cations with Al^{3+}, enhancing the clay's adsorption efficiency for organic compounds. The bentonite structure, consisting of an octahedral alumina sheet between two tetrahedral silica sheets, allows for stacked units, improving adsorptive properties. The introduction of surfactants like CTAB increases the clay's affinity for organic pollutants by replacing inorganic cations and enhancing adsorption. The layered structure provides a high surface area and ample interlayer spacing, beneficial for adsorption processes [32]. These findings align with standard reference patterns from the Joint Committee on Powder Diffraction Standards (JCPDS), specifically numbers 88-1175 and 84-1286. SEM micrographs (Figures 3a, 3b, 3c, and 3d) reveal distinct morphological differences between Clay/TiO_2 and Clay/TiO_2/CTAB. The intercalation of clay and TiO_2 resulted in a structure where the TiO_2 was dispersed rather than uniformly mixed, with TiO_2 particles primarily adhering to the clay surface and prone to detachment.

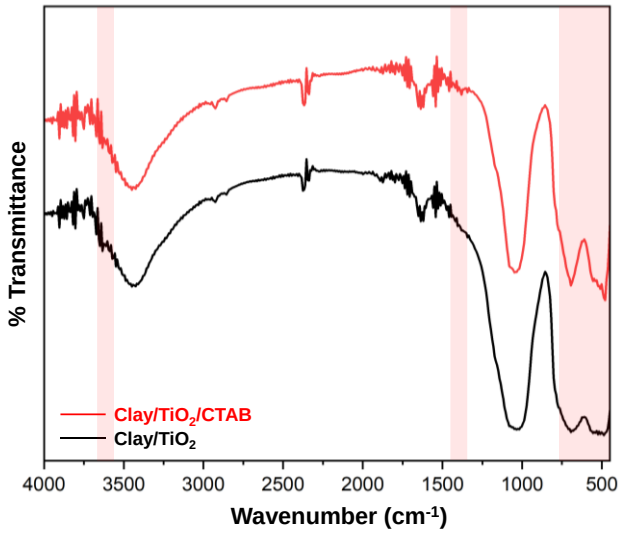

Fig. 1. FTIR spectrum of synthesized materials (Clay/TiO_2 and Clay/TiO_2/CTAB).

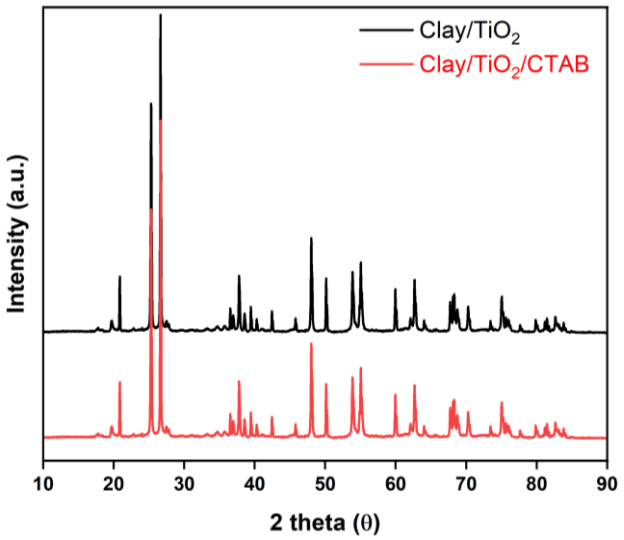

Fig. 2. XRD pattern of synthesized materials (Clay/TiO_2 and Clay/TiO_2/CTAB).

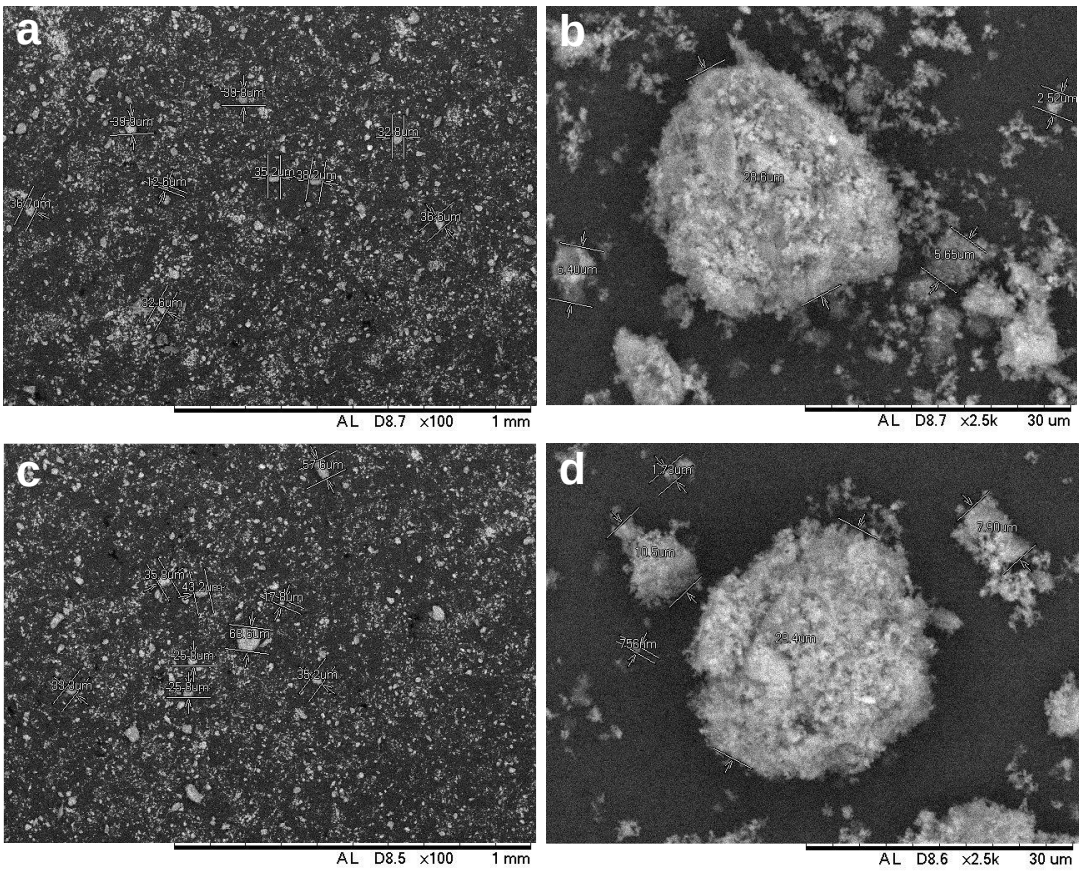

Fig. 3. SEM images of synthesized materials: (a,b) Clay/TiO_2 and (c,d) Clay/TiO_2/CTAB.

Although the activated clay exhibited good porosity and a porous spherical morphology that served as an effective template for TiO_2, the binding was suboptimal compared to Clay/TiO_2/CTAB. This resulted in a less stable structure where TiO_2 particles could easily detach. The porosity of activated clay, with its spherical morphology, provided a good template for TiO_2 deposition, but

the absence of a strong binding agent limited the composite's structural integrity.

Meanwhile, the inclusion of the CTAB surfactant in Clay/TiO_2 enhanced particle agglomeration and improved the attachment of TiO_2 to the clay. CTAB acted as a pillarizing agent, increasing the basal spacing of the clay and facilitating the incorporation of TiO_2 into the clay's lattice. This process, known as surfactant-assisted intercalation, improved the dispersion and attachment of TiO_2, resulting in a more stable and efficient composite material. This augmentation significantly benefited the photocatalytic process, increasing the clay's surface area by allowing CTAB to insert into the clay's pore lattice, creating a pillarized structure filled with TiO_2. These observations confirmed the successful incorporation of clay/TiO_2 particles with the CTAB surfactant.

3.3. Removal of MO by adsorption over Clay/TiO_2/CTAB

The degradation of MO using Clay/TiO_2/CTAB was systematically evaluated with various experimental parameters, including pH optimization, contact time, and the influence of concentration. Initially, the optimization of pH was carried out to determine the optimal conditions for the degradation of the MO compound. According to Figure 4, the Clay/TiO_2/CTAB composite achieved peak efficiency at a pH of 5, exhibiting a degradation capacity of 43.23 mg/g and a degradation efficiency of 87.84%. This data indicated that the Clay/TiO_2/CTAB composite was more effective at degrading MO under acidic conditions, particularly at pH 5, compared to the Clay/TiO_2 system. The enhanced degradation performance in acidic environments could be attributed to the protonation of nitrogen double bonds within the MO structure, facilitated by the presence of hydrogen ions.

This protonation induced a resonation effect, rendering the MO molecule positively charged and more susceptible to degradation processes. In addition, the pH of the solution played a crucial role in the photocatalytic degradation of organic pollutants [43]. In acidic conditions, the presence of hydrogen ions (H^+) can protonate functional groups within organic molecules, altering their chemical structure and increasing their susceptibility to oxidative degradation. This phenomenon is particularly significant for compounds like MO, where protonation of nitrogen double bonds can enhance the effectiveness of photocatalysts by increasing the adsorption and reaction rates on the catalyst surface [44].This study investigated the impact of contact time on the degradation capacity of MO using a Clay/TiO_2/CTAB composite material. Experiments were conducted at an optimum pH of 5, with a constant MO concentration of 25 mg.L^{-1}, and varied contact times of 30, 60, 90, 120, and 150 minutes.

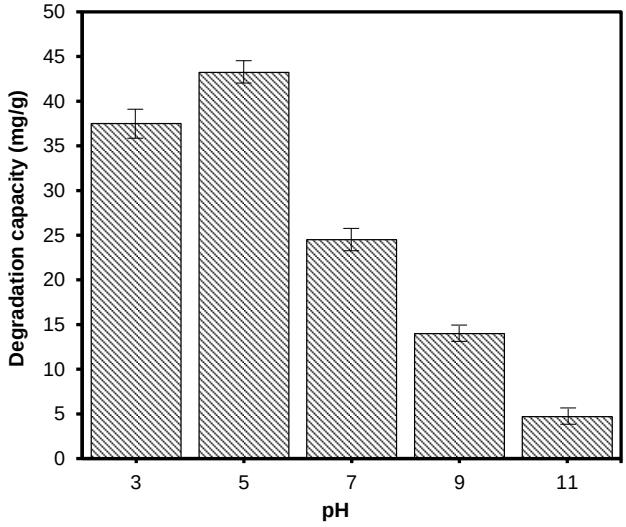

Fig. 4. Effect of pH on MO degradation capacity using Clay/TiO_2/CTAB.

The results, as illustrated in Figure 5, reveal a notable increase in degradation capacity from 30 to 60 minutes, attributable to the freshness of the material and the absence of water contamination. Initially, the degradation ability was enhanced, peaking at 60 minutes; however, it subsequently declined from 90 to 150 minutes due to material saturation, resulting in diminished adsorption-photodegradation efficiency.

The findings indicated that the optimal contact time for the Clay/TiO_2/CTAB material was 60 minutes, achieving a maximum degradation capacity of 44.25 mg/g and an efficiency of 89.90% (Figure 5a). The initial increase in degradation capacity was linked to the availability of active sites and the inherent porosity of the material, which were not yet occluded by other compounds [45]. Figure 5b displays the reaction kinetics data based on pseudo-order one to show the adsorption speed of the Clay/TiO_2/CTAB composite. The data showed that the 30th minute to 60th minute had a good adsorption speed with the movement of the Ln(C0/Ct) value decreasing. In contrast, the degradation time from 60 to 150 minutes increased due to the decrease in the adsorption-photodegradation ability of the composite. Conversely, as the material became saturated, its capacity to adsorb pollutants decreased. This saturation effect is commonly observed in porous materials used for adsorption and photocatalytic processes, where prolonged exposure to contaminants reduces the effectiveness of active sites [46]. The prolonged contact time can lead to surface saturation, where active sites become occupied by pollutant molecules, reducing the efficiency of the photocatalytic process. This phenomenon is influenced by factors such as the surface area, pore structure, and surface chemistry of the photocatalyst material, as well as the concentration and nature of the pollutants [45, 46].

The final experiment evaluated the degradation capacity of the Clay/TiO_2/CTAB composite for MO across concentrations of 20, 25, 30, and 35 $mg.L^{-1}$, with a fixed contact time of 60 minutes at an optimal pH of 5. The results, depicted in Figure 6, demonstrated enhanced degradation capabilities at lower concentrations of 20 and 25 $mg.L^{-1}$. This improvement could be attributed to factors such as reduced competition for active sites, increased penetration ability, the dynamics of adsorption isotherms, and the effects of surface saturation on the Clay/TiO_2/CTAB material.

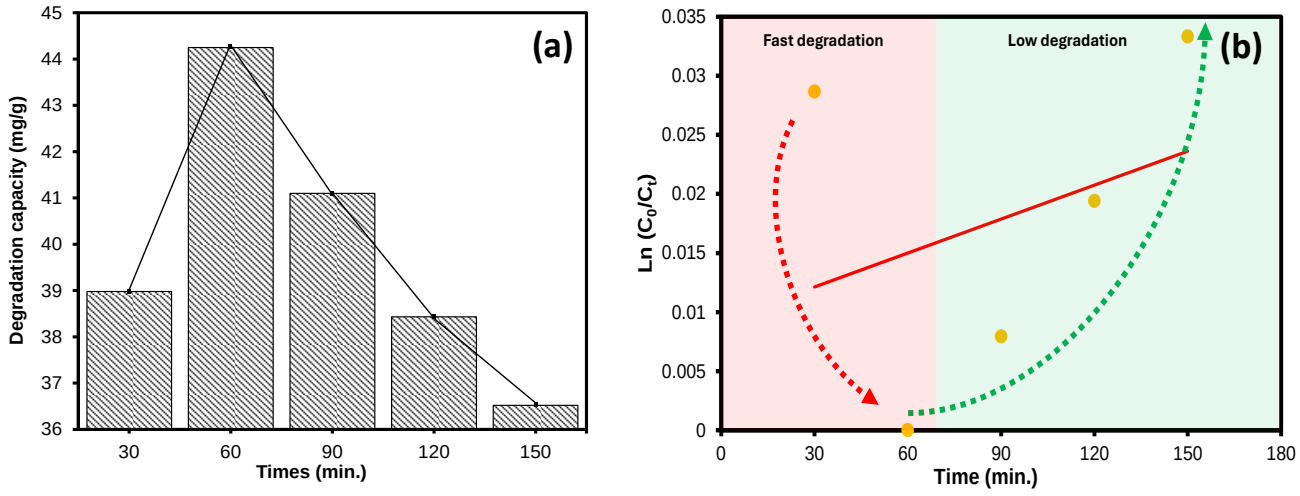

Fig. 5. The adsorption-photodegradation test: (a) contact time test for the Clay/TiO_2/CTAB material and (b) Kinetics rate of Clay/TiO_2/CTAB.

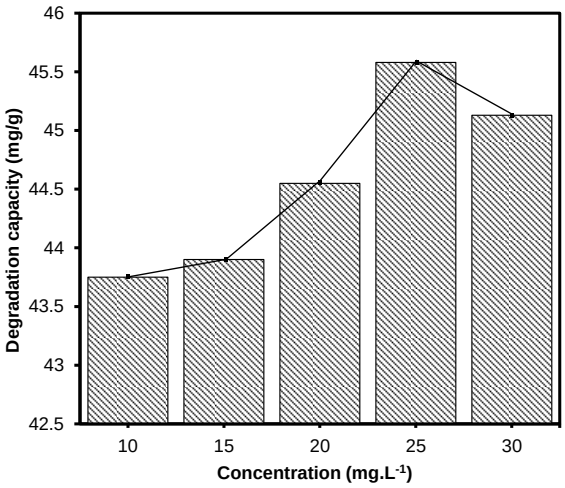

Fig. 6. Degradation capabilities using Clay/TiO_2/CTAB.

This phenomenon is governed by adsorption isotherms, which describe the relationship between the concentration of pollutants in solution and the amount adsorbed onto the catalyst surface. At lower pollutant concentrations, fewer molecules compete for the available active sites on the adsorbent surface, facilitating more effective adsorption [43]. The highest degradation capacity was observed at a concentration of 25 mg/L, achieving 45.58 mg/g with a degradation efficiency of 92.60%. In contrast, at 30 mg/L, the degradation performance declined due to saturation of the active sites within the Clay/TiO_2/CTAB material or excessive solution density, causing the clay to float, which adversely affected the degradation process and reduced the efficiency. Surface saturation occurred when all active sites on the catalyst surface were occupied by pollutant molecules, limiting further adsorption and degradation capacity. Additionally, factors such as solution density and the clay particles' buoyancy could affect the photocatalytic process's stability and efficiency [44]. These findings suggested that the Clay/TiO_2/CTAB composite exhibited a robust ability to degrade MO, particularly effective at lower concentrations, highlighting its potential for treating organic colour compounds in wastewater. Table 1 presents an overview of the degradation characteristics of MO when treated with a composite of Clay/TiO_2/CTAB under varying experimental conditions. It highlights key parameters such as initial MO concentration (25 mg/L), optimal pH (5), and contact time (60 minutes) to achieve a maximum degradation capacity of 45.58 $mg.L^{-1}$ with an impressive efficiency of 92.60%. The data revealed that the degradation process was significantly enhanced in acidic conditions where protonation of nitrogen double bonds in MO increased the susceptibility to degradation reactions. Furthermore, the data indicated that as the concentration of MO rose, the degradation efficiency declined due to surface saturation of the adsorbent material, thus limiting its capacity to adsorb further pollutants.

Figure 7 illustrates the photodegradation process of a Clay/TiO_2/CTAB composite under visible light illumination, highlighting the catalytic degradation of pollutants over time. Initially, the layered composite structure, consisting of clay as a support, TiO_2 as a photocatalyst, and CTAB as a surfactant, was exposed to visible light. The TiO_2 component was activated, generating electron-hole pairs that facilitated the breakdown of organic pollutants. As the reaction progressed, a noticeable reduction in pollutant concentration was observed, with maximum degradation efficiency occurring at 60 min. The process became less efficient after this point, as shown by the decline in degradation rate over time. This suggested an optimal duration for the visible-light-induced photocatalytic activity of the Clay/TiO_2/CTAB composite.

Table 1. The summary of the adsorption-photodegradation of MO dye.

Parameter	Description	Value
MO concentration	Initial concentration of MO compound	25 mg.L^{-1}
Optimal contact time	Optimal time for the adsorption process	60 min
Degradation capacity	Maximum degradation capacity by the adsorbent	45.58 mg.L^{-1}
Degradation efficiency	Percentage of degradation achieved	92.60%
Optimal pH	Acidity level that enhances efficiency	5
Degradation capacity at pH	At pH 5, degradation capacity	43.23 mg.L^{-1}
Degradation efficiency at pH	Efficiency at pH 5	87.84%
Degradation capacity at contact time	Maximum at 60 min.	44.25 mg.L^{-1}
Degradation efficiency at contact time	Maximum efficiency during 60 min.	89.90%
Variations in MO concentration	Capacity tested at concentrations of 20-35 mg.L^{-1}	20 mg.L^{-1} and 25 mg.L^{-1}
Kinetics Rate (k)	Performance evaluation to degrade MO (Pseudo-First-Order Kinetics)	9.57 × 10^{-5} min^{-1}

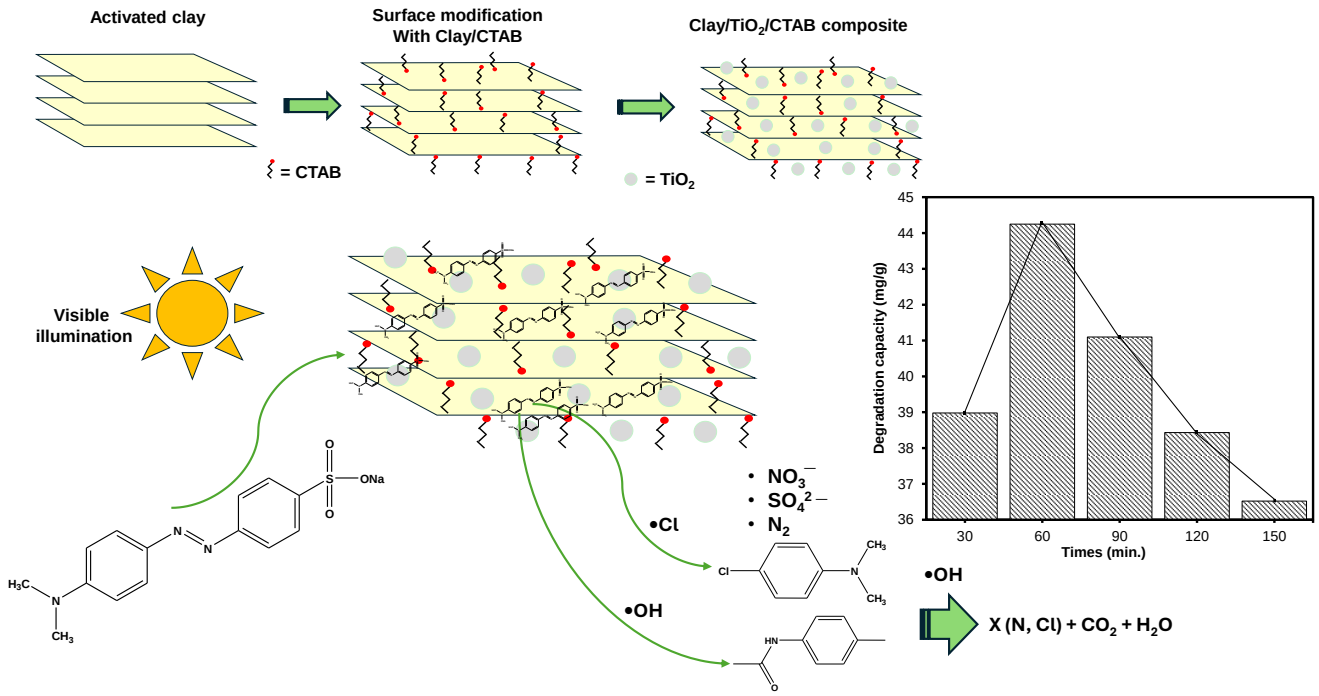

Fig. 7. The adsorption-photodegradation process of a Clay/TiO_2/CTAB composite over MO compound.

4. Conclusions

Clay/TiO_2/CTAB demonstrates significant capabilities in the adsorption-photodegradation of MO colour compound. TiO_2-P25 exhibits excellent integration in forming the Clay/TiO_2/CTAB composite. The synergistic interaction among the materials results in optimal degradation performance at a concentration of 25 mg.L^{-1}, achieving a degradation capacity of 45.58 mg/g and a degradation efficiency of 92.60%. Additionally, the degradation capacity at a pH of 5 reaches its peak at a concentration of 2 mM for methyl orange dye solution, with a degradation capacity of 43.23 mg/g and a degradation efficiency of 87.84%. Furthermore, at a contact time of 60 minutes, the degradation capacity is measured at 44.25 mg.L^{-1}, corresponding to a degradation efficiency of 89.90%. The effectiveness of clay in mitigating waste pollution

holds considerable promise for environmentally friendly materials.

Acknowledgements

The author sincerely thanks the National Institute of Technology Raipur for their generous provision of an institutional research fellowship, which offers valuable technical and financial support.

References

[1] Basuki, T. M., Indrawati, D. R., Nugroho, H. Y. S. H., Pramono, I. B., Setiawan, O., Nugroho, N. P., ... Savitri, E. (2024). Water Pollution of Some Major Rivers in Indonesia: The Status, Institution, Regulation, and Recommendation for Its Mitigation. Polish Journal of Environmental Studies, 33(4), 3515–3530. https://doi.org/10.15244/pjoes/178532

[2] Umami, A., Sukmana, H., Wikurendra, E. A., & Paulik, E. (2022). A review on water management issues: potential and challenges in Indonesia. Sustainable Water Resources Management, 8(3), 63. https://doi.org/10.1007/s40899-022-00648-7

[3] Hayati, A., Wulansari, E., Armando, D. S., Sofiyanti, A., Amin, M. H. F., & Pramudya, M. (2019). Effects of in vitro exposure of mercury on sperm quality and fertility of tropical fish Cyprinus carpio L. The Egyptian Journal of Aquatic Research, 45(2), 189–195. https://doi.org/10.1016/j.ejar.2019.06.005

[4] Wulan, D. R., Hamidah, U., Komarulzaman, A., Rosmalina, R. T., & Sintawardani, N. (2022). Domestic wastewater in Indonesia: Generation, characteristics and treatment. Environmental Science and Pollution Research International, 29(22), 32397. https://doi.org/10.1007/s11356-022-19057-6

[5] Kishor, R., Purchase, D., Saratale, G. D., Saratale, R. G., Ferreira, L. F. R., Bilal, M., ... Bharagava, R. N. (2021). Ecotoxicological and health concerns of persistent coloring pollutants of textile industry wastewater and treatment approaches for environmental safety. Journal of Environmental Chemical Engineering, 9(2), 105012. https://doi.org/10.1016/j.jece.2020.105012

[6] Ahmed, J., Thakur, A., & Goyal, A. (2021). Industrial wastewater and its toxic effects. In Chemistry in the Environment Biological Treatment of Industrial Wastewater (pp. 1–14). https://doi.org/10.1039/9781839165399-00001

[7] Islam, T., Repon, M. R., Islam, T., Sarwar, Z., & Rahman, M. M. (2023). Impact of textile dyes on health and ecosystem: A review of structure, causes, and potential solutions. Environmental Science and Pollution Research, 30(4), 9207–9242. https://doi.org/10.1007/s11356-022-24398-3

[8] Al-Tohamy, R., Ali, S. S., Li, F., Okasha, K. M., Mahmoud, Y. A.-G., Elsamahy, T., ... Sun, J. (2022). A critical review on the treatment of dye-containing wastewater: Ecotoxicological and health concerns of textile dyes and possible remediation approaches for environmental safety. Ecotoxicology and Environmental Safety, 231, 113160. https://doi.org/10.1016/j.ecoenv.2021.113160

[9] Muzakkar, M. Z., Umar, A. A., Ilham, I., Saputra, Z., & Zulfikar, L. (2019). Chalcogenide material as high photoelectrochemical performance Se doped TiO_2/Ti electrode: Its application for Rhodamine B degradation. Journal of Physics: Conference Series, 1242, 1–8. https://doi.org/10.1088/1742-6596/1242/1/012016

[10] Maulidiyah, M., Wijawan, I. B. P. B. P., Wibowo, D., Aladin, A., Hamzah, B., & Nurdin, M. (2018). Photoelectrochemical Performance of TiO_2/Ti Electrode for Organic Compounds. IOP Conference Series: Materials Science and Engineering, 367(1), 012060. https://doi.org/10.1088/1757-899X/367/1/012060

[11] Roosmini, D., Andarani, P., & Nastiti, A. (2010). Heavy metals (Cu and Cr) pollution from textile industry in surface water and sediment (Case study: Cikijing River, West Java, Indonesia). In The 8th international symposium on Southeast Asian water environment. https://www.academia.edu/download/53007945/

[12] Sihombing, A. K. (2020). Penegakan hukum terhadap pencemaran lingkungan di Sungai Cikijing, Jawa Barat akibat aktivitas industri tekstil PT. Kahatex. Jurnal Hukum Lingkungan Indonesia, 7(1), 98–117. https://doi.org/10.38011/jhli.v7i1.209

[13] Suriadikusumah, A., Mulyani, O., Sudirja, R., Sofyan, E. T., Maulana, M. H. R., & Mulyono, A. (2021). Analysis of the water quality at Cipeusing river, Indonesia using the pollution index method. Acta Ecologica Sinica, 41(3), 177–182. https://doi.org/10.1016/j.chnaes.2020.08.001

[14] Roosmini, D., Septiono, M. A., Putri, N. E., Shabrina, H. M., Salami, I. R. S., & Ariesyady, H. D. (2018). River water pollution condition in upper part of Brantas River and Bengawan Solo River. In IOP Conference Series: Earth and Environmental Science (Vol. 106, p. 12059). IOP Publishing. https://doi.org/10.1088/1755-1315/106/1/012059

[15] Esho, H. (2015). Dynamics of the Textiles & Apparel Industries in Southeast Asia-A Preliminary Analysis. Journal of International Economic Studies, 29(1), 85–106. https://doi.org/10.15002/00011120

[16] Natsir, M., Putri, Y. I., Wibowo, D., Maulidiyah, M., Salim, L. O. A., Azis, T., ... Nurdin, M. (2021). Effects of Ni–TiO_2 pillared Clay–Montmorillonite composites for photocatalytic enhancement against reactive orange under visible light. Journal of Inorganic and Organometallic Polymers and Materials, 31(8), 3378–3388. https://doi.org/10.1007/s10904-021-01980-9

[17] Wibowo, D., Muzakkar, M. Z., Saad, S. K. M., Mustapa, F., Maulidiyah, M., Nurdin, M., & Umar, A. A. (2020). Enhanced visible light-driven photocatalytic degradation supported by Au-TiO_2 coral-needle nanoparticles. Journal of Photochemistry and Photobiology A: Chemistry, 398. https://doi.org/10.1016/j.jphotochem.2020.112589

[18] Hikmawati, Watoni, A. H., Wibowo, D., Maulidiyah, & Nurdin, M. (2017). Synthesis of Nano-Ilmenite ($FeTiO_3$) doped TiO_2/Ti Electrode for Photoelectrocatalytic System. IOP Conference Series: Materials Science and Engineering, 267(1), 012005. https://doi.org/10.1088/1757-899X/267/1/012005

[19] Wibowo, D., Sufandy, Y., Irwan, I., Azis, T., Maulidiyah, M., & Nurdin, M. (2020). Investigation of nickel slag waste as a modifier on graphene-TiO_2 microstructure for sensing phenolic compound. Journal of Materials Science: Materials in Electronics, 1–9. https://doi.org/10.1007/s10854-020-03996-2

[20] Nurdin, M., Muzakkar, M. Z., Maulidiyah, M., Maulidiyah, N., & Wibowo, D. (2016). Plasmonic Silver—N/TiO_2 Effect on Photoelectrocatalytic Oxidation Reaction. J. Mater. Environ. Sci, 7(9), 3334–3343. http://www.jmaterenvironsci.com/Document/vol7/vol7_N9/344-JMES-2470-Nurdin.pdf

[21] Nurdin, M., Zaeni, A., Rammang, E. T., Maulidiyah, M., & Wibowo, D. (2017). Reactor design development of chemical oxygen demand flow system and its application. Analytical and Bioanalytical Electrochemistry, 9(4), 480–494. https://www.researchgate.net/profile/Dwiprayogo-Wibowo/publication/318786548

[22] Muhammad Nurdin, Wibowo, D., Azis, T., Safitri, R. A., Maulidiyah, M., Mahmud, A., ... Umar, A. A. (2022). Photoelectrocatalysis Response with Synthetic Mn–N–TiO_2/Ti Electrode for Removal of Rhodamine B Dye. Surface Engineering and Applied Electrochemistry, 58(2), 125–134. https://doi.org/10.3103/S1068375522020077

[23] Wibowo, D., Mustapa, F., Fabian, A., Fitaloka, E. R., Ardiansyah, D., Adami, A., ... Abriansyah, A. (2024). Highly Adsorption-Photocatalytic Tablet-Shaped Graphite Oxide-TiO_2 Composites for Handling Organic Dye Pollutants. Journal of Chemical and Petroleum Engineering, 58(1), 1–16. https://doi.org/10.22059/jchpe.2024.370403.1475

[24] Wibowo, D., Mustapa, F., Mukaddas, J., Nakai, T., Alfandi, R., Assidieq, M., ... Nurdin, M. (2024). Dual-functional graphite/TiO_2 nanocomposites for high-efficiently adsorption-photoelectrocatalytic degradation. In AIP Conference Proceedings (Vol. 2927, p. 020010). AIP Publishing. https://doi.org/10.1063/5.0192120

[25] Shindhal, T., Rakholiya, P., Varjani, S., Pandey, A., Ngo, H. H., Guo, W., ... Taherzadeh, M. J. (2021). A critical review on advances in the practices and perspectives for the treatment of dye industry wastewater. Bioengineered, 12(1), 70–87.

https://doi.org/10.1080/21655979.2020.1863034

[26] Rice, R. G. (1996). Applications of ozone for industrial wastewater treatment—a review. Ozone: science & engineering, 18(6), 477–515. https://doi.org/10.1080/01919512.1997.10382859

[27] Wibowo, D., Jurumai, L. P., Liawaty, S., Ardi, M., Saida, N. R. R., Rosdiana, R., ... Biddinika, M. K. (2023). Graphite Coupled with TiO_2 Paste Photoelectrodes Well Oriented over COD Photoelectrocatalysis for Rapid Detection of Methylene Blue Organic Dye. Journal of Environmental Engineering, 149(11), 4023070. https://doi.org/10.1061/JOEEDU.EEENG-7354

[28] Maulidiyah, Nurdin, M., Wibowo, D., & Sani, A. (2015). Nano Tube Titanium Dioxide/ Titanium Electrode Fabrication with Nitrogen and Silver Metal Doped Anodizing Method : Performance Test of Organic Compound Rhodamine B Degradation. Pharmacy and Pharmaceutical Sciences, 7(6), 141–146.

[29] Ijaz, M., & Zafar, M. (2021). Titanium dioxide nanostructures as efficient photocatalyst: Progress, challenges and perspective. International Journal of Energy Research, 45(3), 3569–3589. https://doi.org/10.1002/er.6079

[30] Dharma, H. N. C., Jaafar, J., Widiastuti, N., Matsuyama, H., Rajabsadeh, S., Othman, M. H. D., ... Nasir, A. M. (2022). A review of titanium dioxide (TiO_2)-based photocatalyst for oilfield-produced water treatment. Membranes, 12(3), 345. https://doi.org/10.3390/membranes12030345

[31] Maulidiyah, Azis, T., Nurwahidah, A. T. A. T., Wibowo, D., & Nurdin, M. (2017). Photoelectrocatalyst of Fe co-doped N-TiO_2/Ti nanotubes: Pesticide degradation of thiamethoxam under UV–visible lights. Environmental Nanotechnology, Monitoring & Management, 8, 103–111. https://doi.org/10.1016/j.enmm.2017.06.002

[32] Ulhaq, I., Ahmad, W., Ahmad, I., Yaseen, M., & Ilyas, M. (2021). Engineering TiO_2 supported CTAB modified bentonite for treatment of refinery wastewater through simultaneous photocatalytic oxidation and adsorption. Journal of Water Process Engineering, 43(July), 102239. https://doi.org/10.1016/j.jwpe.2021.102239

[33] Yuan, L., Huang, D., Guo, W., Yang, Q., & Yu, J. (2011). TiO_2/montmorillonite nanocomposite for removal of organic pollutant. Applied clay science, 53(2), 272–278. https://doi.org/10.1016/j.clay.2011.03.013

[34] Chen, D., Du, G., Zhu, Q., & Zhou, F. (2013). Synthesis and characterization of TiO_2 pillared montmorillonites: Application for methylene blue degradation. Journal of colloid and interface science, 409, 151–157. https://doi.org/10.1016/j.jcis.2013.07.049

[35] Khalaf, H., Bouras, O., & Perrichon, V. (1997). Synthesis and characterization of Al-pillared and cationic surfactant modified Al-pillared Algerian bentonite. Microporous Materials, 8(3–4), 141–150. https://doi.org/10.1016/S0927-6513(96)00079-X

[36] Haounati, R., Ouachtak, H., El Haouti, R., Akhouairi, S., Largo, F., Akbal, F., ... Addi, A. A. (2021). Elaboration and properties of a new SDS/CTAB@ Montmorillonite organoclay composite as a superb adsorbent for the removal of malachite green from aqueous solutions. Separation and Purification Technology, 255, 117335. https://doi.org/10.1016/j.seppur.2020.117335

[37] Ismail, N. H. C., Bakhtiar, N. S. A. A., & Akil, H. M. (2017). Effects of cetyltrimethylammonium bromide (CTAB) on the structural characteristic of non-expandable muscovite. Materials Chemistry and Physics, 196, 324–332. https://doi.org/10.1016/j.matchemphys.2017.05.007

[38] Maulidiyah, M., Natsir, M., Fitrianingsih, F., Arham, Z., Wibowo, D., & Nurdin, M. (2017). Lignin degradation of oil palm empty fruit bunches using TiO_2photocatalyst as antifungal of Fusarium oxysporum. Oriental Journal of Chemistry, 33(6), 3101–3106. https://doi.org/10.13005/ojc/330651

[39] Cardona, Y., Korili, S. A., & Gil, A. (2023). Use of clays and pillared clays in the catalytic photodegradation of organic compounds in aqueous solutions. Catalysis Reviews, 1–48. https://doi.org/10.1080/01614940.2023.2178736

[40] Nayak, P. S., & Singh, B. K. (2007). Instrumental characterization of clay by XRF,

XRD and FTIR. Bulletin of materials science, 30(3), 235–238. https://doi.org/10.1007/s12034-007-0042-5

[41] Wibowo, D., Sumarlin, S., Aridan, A., Herman, S., Murdi, M., Ndibale, W., ... Nurcayah, N. (2023). Testing BIOSEL-SR2020 to Reduce Physical-Chemical Contents in Faecal Sludge Treatment Installations in Puulonggida and Potential as An Organic Fertilizer Ingredient. Jurnal Kesehatan Lingkungan: Jurnal dan Aplikasi Teknik Kesehatan Lingkungan, 20(2), 171–184. https://doi.org/10.31964/jkl.v20i2.663

[42] Mustapa, F., Malik, Z. A., Wibowo, D., Idris, M., Muzakkar, M. Z., Zulfan, A., ... Nurdin, M. (2023). Tailoring sustainable pretreatment materials for reverse osmosis: Banana-peel carbon-TiO_2/Te biocomposites as effective adsorbent. Chemical Engineering Research and Design, 200, 510–520. https://doi.org/10.1016/j.cherd.2023.10.044

[43] Foo, K. Y., & Hameed, B. H. (2010). Insights into the modeling of adsorption isotherm systems. Chemical engineering journal, 156(1), 2–10. https://doi.org/10.1016/j.cej.2009.09.013

[44] Chen, D., Cheng, Y., Zhou, N., Chen, P., Wang, Y., Li, K., ... Zhang, R. (2020). Photocatalytic degradation of organic pollutants using TiO_2-based photocatalysts: A review. Journal of Cleaner Production, 268, 121725. https://doi.org/10.1016/j.jclepro.2020.121725

[45] Chong, M. N., Jin, B., Chow, C. W. K., & Saint, C. (2010). Recent developments in photocatalytic water treatment technology: a review. Water research, 44(10), 2997–3027. https://doi.org/10.1016/j.watres.2010.02.039

[46] Umar, M., & Aziz, H. A. (2013). Photocatalytic degradation of organic pollutants in water. Organic pollutants-monitoring, risk and treatment, 8, 196–197. https://doi.org/10.5772/53699

How to cite this paper:

Nohong, N., Limbong Baratau, J. T., Wibowo, D., Mustapa, F., Zulfan, A., & Muhammad Nurdin, M. M. (2025). Thermal Activation and Loading of Clay/TiO_2/CTAB Composite: Physicochemical Characterization and Adsorption-Photodegradation of Methyl Orange. Advances in Environmental Technology, 11(2), 193-206.DOI: 10.22104/aet.2025.6993.1920